Impact of Antenna Tilting on Propagation Shadowing Model

Dereje W. Kifle and Bernhard Wegmann
Nokia Siemens Networks
Munich, Germany
Emails: {dereje.woldemedhin.ext; bernhard.wegmann@nsn.com}

Ingo Viering
Nomor Research GmbH
Munich, Germany
Email: viering@nomor.de

Anja Klein
Technische Universität Darmstadt
Communications Engineering Lab
Darmstadt, Germany
Email: a.klein@nt.tu-darmstadt.de

***Abstract*—With active antenna systems AAS) cell deployment changes can be handled rather flexible to meet the local and momentary capacity demands. Antenna tilt is one of the important parameters that should be properly adjusted in order to enhance the performance and efficiency of a cellular network. Simulative performance evaluation of these gains currently assumes radio propagation models where the shadowing map remains unchanged with respect to tilt changes. The assumption, however, may not be realistic in particular to dense urban and urban scenarios. This paper investigates the impact of tilt on the shadowing map with regard to the current 3GPP assumptions. Moreover, the work tries to check if the shadowing process can be really assumed as stationary and independent from beam changes. The investigations are based on shadowing maps isolated from real world ray tracing propagation maps and has been carried out for urban scenario with various beam tilt settings.**

***Index Terms*—Radio propagation modeling, Shadowing, AAS**

I. Introduction

The nature of a radio propagation environment determines the performance and efficiency of wireless communication systems. In the course of propagation, a radio wave not only attenuates through distance but also undergoes through different physical phenomenon; i.e. reflection, diffraction and scattering, before arriving at a receiver terminal. Depending on the type of the environment, these effects cause instant fluctuation in signal attenuation level and induce signal fading to a wireless channel making the channel more unpredictable. Fading is mainly caused by multi path effect and shadowing from obstacles in the environment. Radio propagation models, therefore, try to approximate those effects and predict the losses in during signal propagation.

In wireless communications, the dominant propagation loss is due to the attenuation of signal amplitude through distance and this loss is referred as signal path loss PL. In statistical modeling, the local mean value of the path loss $PL(r)$ at a distance r from a transmitter is modeled as a random variable having a log-normal distribution about a mean equal to a path loss component defined solely dependent on distance and is termed as mean area-mean) path loss, i.e. $\overline{PL(r)}$ [1]. $\overline{PL(r)}$ is predicted by path loss models and it is exponentially proportional to the shortest distance r from the transmitter where the exponent value depends on the nature of the propagation environment. In a free space propagation, for example, the path loss exponent is found to be 2 whereas in real outdoor propagation environments its value is between 2 and 4, and it is even higher in complex indoor topologies [1]. The other propagation loss component that gives rise to fluctuation in the signal attenuation level around $\overline{PL(r)}$ is called shadowing S and it is caused by various propagation obstructions. Shadowing map $S(x, y)$ is modeled as log-normally distributed random variable with zero mean. The standard deviation of the shadowing σ_s usually ranges from 5 to 12 dB depending on type of propagation scenarios and the model used to predict the distance dependent path loss component $(\overline{PL(r)})$ [1].

In 3GPP propagation models, the shadowing effect is included as a log-normally distributed random variable with a standard deviation values of 10 and 8 dB for dense urban and urban scenarios respectively [2]. According to the current 3GPP model, the propagation model parameters for the path loss and shadowing model assumptions applies irrespective of antenna tilt settings [2]. While changing antenna tilt values, the model assumes the shadowing statistical behavior is stationary at any point for one antenna and, hence, applies identical shadowing map independent of the tilt. This assumption, however, might be questionable especially in dense urban and urban scenarios where there are many obstructive objects that could change the shadowing behavior with beam tilt variation. This instationarity might result in unpredicted signal level variations in a mobile network and could affect system performance and introduce more inaccuracies where system configuration parameters are sensitive like in adaptive tilt optimization and Self Organizing Network (SON) operation.

In this paper, the 3GPP shadowing propagation model and assumptions are thoroughly investigated considering different antenna tilt settings. The investigation is aimed at checking validity of the 3GPP stationarity assumptions of the shadowing map by extracting shadowing maps from ray tracing propagation maps for various tilt configuration and different sites. Moreover, it has also studied existence of correlations among tilt specific extracted shadowing maps. A propagation map generated by 3GPP propagation modeling and assumptions is used as a reference and validation of the approach.

This paper is organized as follows. The state of the art of 3GPP urban propagation models is described in Section

II. Section III describes ray tracing prediction approach and scheme adopted here. The approach employed to extract shadowing map and used optimization techniques to determine the mean distance-dependent path loss and antenna backward attenuation are discussed in Section IV. Section V evaluates the results and shows analysis. The last section, Section VI, concludes the work.

II. 3GPP Urban Propagation Model

This section describes the state of the art in 3GPP urban propagation models including path loss, shadowing and antenna radiation pattern model.

A. Mean Path Loss

3GPP has developed several path loss models for various propagation environment based on measurement data [2]. For the urban environments, the macro cell mean path loss at a distance r from a base station ($\overline{PL(r)}$) is defined as a function of the carrier frequency f_c [MHz], the antenna height above rooftop $\triangle h$ [m] and separation distance r in [km] and it is given by equation (1) [3].

$$\begin{aligned}\overline{PL(r)} = 21 \cdot \log_{10}(f_c) + 80 - 18 \cdot \log_{10}(\triangle h) \\ +40 \cdot [1 - 4 \cdot 10^{-3} \cdot \triangle h] \cdot \log_{10}(r)\end{aligned} \quad (1)$$

B. Propagation Shadowing

The shadowing effect causes signal fading and it results in fluctuation of the total path attenuation level around the mean path loss, $\overline{PL(r)}$. It has been demonstrated from statistics that, this fluctuation is characterized by having a log-normal distribution with zero mean and a standard deviation that depends on propagation environment. Moreover, due to the slow fading process over distance, the model assumes that shadowing values of adjacent locations are correlated and its normalized autocorrelation is approximated and given by [2];

$$R(\triangle x) = e^{-\frac{\triangle x}{d_{cor}}} \quad (2)$$

where $\triangle x$ is the spatial separation between two pixels and the decorrelation distance (d_{cor}) defined as the smallest distance gap where the autocorrelation falls to e^{-1}. In 3GPP shadow modeling, the correlation effect is taken into account with assumptions that shadowing correlation factor of 0.5 exists for shadowing maps between different sites and correlation factor of 1.0 among different sectors on a same site [3].

C. Antenna Radiation Pattern

The vertical and horizontal antenna radiation pattern data, i.e. the two-dimensional $(2D)$ patterns, provided by manufacturers apply only to reflection free environments [4]. The vertical antenna pattern is defined as $B_V(\theta)$ for $-90 \leq \theta \leq 90$ in a vertical plane while horizontal pattern, $B_H(\phi)$, defines the pattern change in the horizontal plane where $-180 \leq \phi \leq 180$. Practically, obstructing and reflecting objects in antenna environment could have an impact and alter this radiation pattern [4]. This requires having an enhanced model that takes this effect into account and accurately estimates the radiation pattern. Furthermore, the $2D$ patterns alone are not enough to determine antenna pattern gain for a point of interest at any position in the network. Conventionally, a quasi $3D$ pattern $B_{3D}(\phi, \theta)$ can be generated by linearly combining the $B_H(\phi)$ and $B_V(\theta)$ patterns [5]. With this approach, acceptable total pattern can be obtained for limited angular range in the direction of the main lobe, but it can not accurately reproduce $B_{3D}(\phi, \theta)$ at far field and the backside of the antenna [5]. As a consequence, different novel techniques and approaches have been proposed to account these errors and accurately approximate the $3D$ pattern from the $B_H(\phi)$ and $B_V(\theta)$ via interpolation [6] [7] [8]. In accordance with this, for mobile network simulation scenarios, 3GPP has defined the azimuth and elevation patterns as shown in [3] and the $3D$ pattern can be approximated as depicted in equations (3) and (4) [9].

$$\begin{aligned} B_H(\phi) &= -\min\left\{\xi, 12 \cdot \left(\frac{\phi - \Phi_o}{\Phi_{3dB}}\right)^2\right\} \Rightarrow Azimuth \\ B_V(\theta) &= -\min\left\{\xi, 12 \cdot \left(\frac{\theta - \Theta_t}{\Theta_{3dB}}\right)^2\right\} \Rightarrow Elevation \end{aligned} \quad (3)$$

$$B_{3D}(\phi, \theta) = -\min\left\{\xi, -\left[B_H(\phi) + B_V(\theta)\right]\right\} \quad (4)$$

In the above equations, Φ_{3dB} and Θ_{3dB} are the half power $(3dB)$ bandwidths of the main lobe in the horizontal and vertical plane respectively, while Φ_o gives the azimuth orientation and Θ_t represents vertical tilt angle. In the pattern model given above, ξ is a factor introduced to provide total backward attenuation that takes impact of propagation conditions into account. ξ is optimized to 25dB [2] and it is commonly adopted in simulation scenarios. However, this may not necessarily reflect the accurate total pattern and this value could diverge depending on the clutter type of the considered scenario.

According to the current 3GPP model and assumptions, a change of tilt settings causes a change in the received power level at any (x, y) location in the network which is equal to the observed antenna gain pattern difference $(\Delta B_{3D}(x, y))$ with respect to the same (x, y) position, i.e $\Delta P_{rx}(x, y) = \Delta B_{3D}(x, y)$ whereas, the shadowing map $(s(x, y))$ is assumed to be invariable with tilt.

III. Ray Tracing Propagation Map Data

For the investigation, a propagation map data generated by a network planning tool based on ray tracing approach has been considered. The tool employs $3D$ models and urban clutter behaviors in order to include more real life propagation effects and to be able to predict propagation maps with high accuracy. In ray tracing approach, despite the fact that considering several rays and paths provides the possibility to take multiple paths effect into account, it is computationally more expensive and put constraint on the available tools. It has been nevertheless shown that a ray tracing prediction technique made using one ray only on the dominant path between the transmitter and receiver performs with an accuracy as

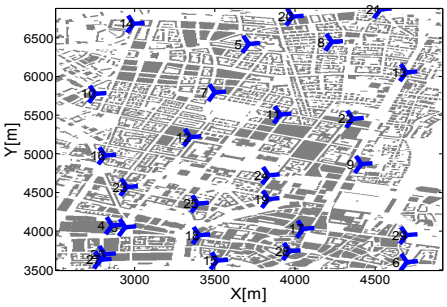

Fig. 1. Network Layout: Munich urban scenario

TABLE I
BASIC SYSTEM PARAMETER SETTINGS.

Parameter	Settings
Tool used to generate propagation map	Ray Tracing tool (WinProp)
Urban Scenario - City	Munich
Network Size	27 tri-sectored, i.e 81 cells
Antenna Total Power	43 dBm
Antenna gain	14.5 dBi
Antenna HPBW settings	$\phi_{3dB} = 65^{\circ}$ and $\theta_{3dB} = 25^{\circ}$
Grid resolution	$5m \times 5m$
Tilt angle Values	$[4^{\circ}, 6^{\circ}, 10^{\circ}, 14^{\circ}]$

high as the path loss prediction that uses several rays. This is demonstrated in the work [10], [11] where performance evaluation was done between the full ray tracing and the dominant path approaches. Hence, a Dominant path Prediction Model (DPM) setting is utilized in our tool to generate an outdoor propagation map.

Urban outdoor propagation scenario is studied in our investigation. A network layout consisting of 27 tri-sectored sites, i.e. 81 sectors, is considered for city of Munich where the site plan and system parameters configuration settings are done based on realistic site deployment. Figure 1 presents the layout and site locations. Basic settings are summarized in Table I.

IV. EXTRACTION OF SHADOWING MAPS

In this section, empirical modeling technique is used in order to predict the mean path loss. An optimization approach that has been applied in approximating the backward attenuation factor for the radiation pattern model is also presented. Moreover, the scheme of extracting shadowing statistics and investigation approach employed to analyze impact of a tilt is demonstrated.

A. Path Loss Prediction Based on Optimized Antenna Backward Attenuation Factor

In order to extract the shadowing map from the ray tracing propagation data, the correct propagation loss parameter values that would estimate the losses contributed by the mean path loss and antenna gain pattern variation is needed. Due to the fact that each sector experiences different propagation clutter type in the direction of their serving antenna, the propagation parameters would have different path loss coefficients and antenna backward attenuation factors.

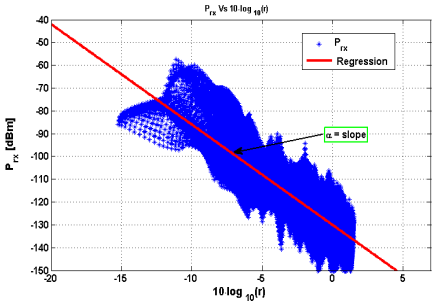

Fig. 2. Measured Received Power Values over distance (r) [km]: [P_{rx} Vs $10 \cdot log_{10}(r)$]

1) Empirical Path Loss Prediction: Despite the complex factors determining the total propagation loss, the mean path loss can be empirically approximated from the trend and variation of signal attenuation level through distance. The most popular and widely used path loss model is Hata's propagation model which was formulated based on intensive measurement data [3], [12]. Accordingly, the distance dependent mean path loss, $\overline{PL(r)}$, is represented in a generic formula [12], [13]:

$$\overline{PL(r)} = A + \alpha \cdot 10 \cdot \log_{10}(r) \quad (5)$$

where A represents a path loss offset and α approximates path loss exponent. Usually the path loss is represented with two coefficients, the path loss offset (A) and a parameter B that includes the path loss exponent term, i.e., $B = \alpha \cdot 10$. Hence, the path loss is usually expressed with those coefficients in the form of $\overline{PL(r)} = A + B \cdot \log_{10}(r)$. As illustrated in equation 1, these path loss coefficients are functions of frequency, base station height and distance [3], [12], [13], [14]. The ray tracing data is exploited to empirically predict the path loss coefficients. Regression is applied and linear curve fitting approach is utilized on the measured propagation values $P_{rx}[dBm]$ Vs $10 \cdot log_{10}(r)[dB]$, as shown in Figure 2, r is given in km. Since sectorized antenna systems are employed, the propagation maps P_{rx} values include the effect of antenna radiation pattern loss and this may lead to inaccurate path loss coefficient prediction. Therefore, the impact of radiation pattern should be excluded from the P_{rx} statistics [14] before applying regression, $P_{rx}(x, y)$ - $B_{3D}(x, y)$); nevertheless, the $B_{3D}(x, y)$ should be properly evaluated which in turn requires optimal value of ξ in the radiation pattern model.

2) Optimization Approach: As explained in section II, antenna backward attenuation factor ξ could be impacted by nearby objects and it may vary for different sectors in a network. Accurately predicted path loss model must result and confirm the normally distributed shadowing model assumption with a zero mean and minimum standard deviation [1]. Accordingly, the value of the standard deviation is used to optimize ξ. A brute-force based optimization approach is carried out for a wide range of ξ values and hence, a cost function f_{σ_s} is defined from the shadowing standard deviation $\sigma_{(s,t)}$ which is evaluated at each sector and for different

tilt setting t. f_{σ_s} is a function of the predicted path loss coefficients for each ξ configuration, $A(\xi)$ and $B(\xi)$, and it is given by:

$$f_{\sigma_s}(\xi, A(\xi), B(\xi)) = \frac{1}{T}\sum_{t=1}^{T}\sigma_{(s,t)}, \tag{6}$$

where the parameter T stands for the number of considered tilt setting values and used here to average out the standard deviation evaluated for all T tilts at each cell.

B. Extracting Shadowing Map

Based on the predicted path loss and antenna radiation pattern loss values, the large scale propagation loss attributed to shadowing is extracted from the the ray tracing propagation map as follows:

$$\begin{aligned} S_c(\xi, A(\xi), B(\xi), t) = P_{tx} - P_{rx} + G_{dBi} \\ + B_{3D}(\phi, \theta)_t - \overline{PL(r)}, \end{aligned} \tag{7}$$

where, S_c is the shadowing map in dB, P_{tx} and P_{rx} are the transmit and received power levels respectively. The term G_{dBi} gives the dBi gain of the antenna.

V. Evaluation of Extracted Shadowing Map

Applying various tilt settings, optimization has been carried out to predict the propagation model parameters (ξ, A and B) and shadowing map is extracted from propagation map of each sector of the considered scenario. Moreover, 3GPP model based generated propagation map has been analyzed and treated the same way to use it as reference and validate feasibility of the approach. Results have demonstrated that changing tilt does not have significant impact on the propagation parameters (A, B) and almost the same propagation parameters have been predicted for a sector irrespective of the tilt.

A. Clutter Specific Propagation Parameters

When applied on the 3GPP model generated propagation map, the employed linear regression path loss approach and optimization has confirmed the same propagation model parameters, i.e. ξ, A, and B, for all sectors network wide as depicted in Figure 3. Whereas for the ray tracing data, those parameters are found to be different for each sectors exhibiting various propagation conditions at specific sectors. This is illustrated in Figure 3 where the path loss exponents are evaluated and presented for each sectors.

B. Statistics of Extracted Shadowing Maps

1) Correlation Property: Shadowing maps extracted from various sectors and tilt settings have confirmed a normal statistical distribution with zero mean and a reasonable value of standard deviation σ_s. Furthermore, while changing tilt, σ_s showed a slight variation leading to comparably closely the same statistical distribution. However, the observed first order statistics alone do not reassert that shadowing remain invariable with respect to different tilt settings. One of the interesting statistical behaviors is to evaluate correlation among the

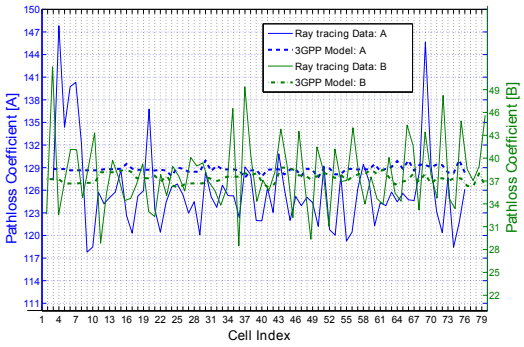

Fig. 3. Predicted path loss coefficients comparison: 3GPP model and Ray tracing data

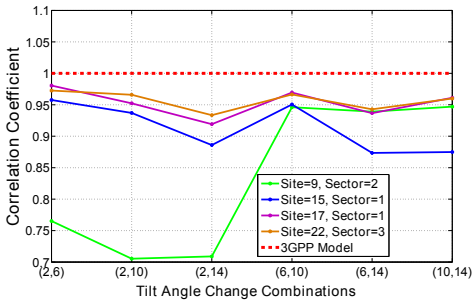

Fig. 4. Shadowing statistics correlation between various tilt settings

shadowing statistics of different tilts. In 3GPP model, shadow map is to be assumed independent of tilt and therefore fully correlated as depicted in Figure 4. Results have demonstrated that statistical correlation still exists but its value is variable depending on the change in the tilt setting exhibiting dependency. This is illustrated in Figure 4 where shadowing correlation coefficients are shown for selected sectors. Furthermore, the assumption of full correlation of shadowing between sectors of the same site in 3GPP could not be confirmed by investigation results.

2) Tilt Dependency of Shadowing: Despite the almost identical first order statistics of the shadowing maps and existence of correlation between the shadowing map statistics among tilts, it is apparent that those do not fully indicate and reflect the shadowing level change that could be experienced at different pixel locations (x, y) in the network. Owing to presence of high building obstructions and reflectors in urban scenarios, while changing antenna tilt from $t = t_k$ to $t = t_z$, the change in received power level at (x, y) pixel position $\Delta P_{rx}(x, y)$ occurs not only due to the perceived change in the radiation pattern, but there could be also suffering from aggressive shadowing objects that might give rise to unpredicted power level drop or vice versa. This has been investigated by looking in to the shadowing level difference $\Delta S(x, y) = S(x, y, t_z) - S(x, y, t_k)$ at each pixel points network wide. Unlike to the 3GPP assumption discussed in section I, it has been found out that $\Delta S(x, y) \neq 0$ and $\Delta P_{rx}(x, y) = \Delta B_{3D}(x, y) + \Delta S(x, y)$ for different tilt change

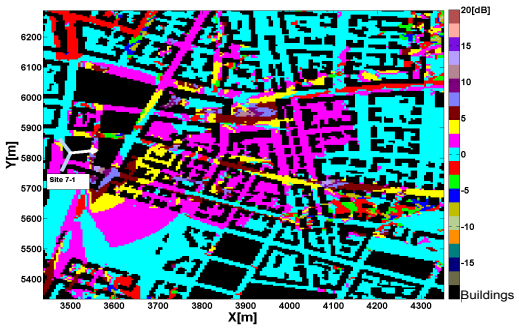

Fig. 5. Shadowing level difference ΔS

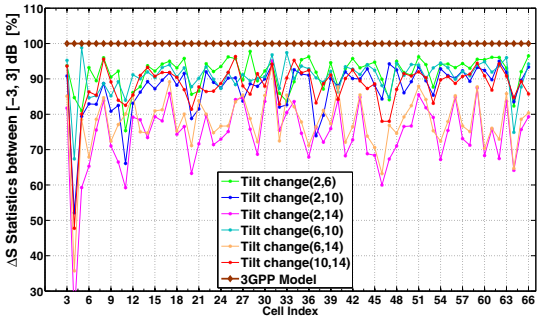

Fig. 6. % of ΔS level statistics between $\pm$3dB

pair (t_k, t_z). This is demonstrated in Figure 5 where ΔS is evaluated for one sector for a tilt change from 2° to 10° for areas in the direction of the main beam. Though a higher tilt is expected to shrink the cell coverage and concentrate signal power close to the base station, the reverse effect has been observed on many of the areas in the sector and this is attributed to the shadowing level variability due to change in tilt. Results have confirmed this in the figure with a significant shadowing level difference at each (x, y) point in the network, for example from 1 - 6 dB, after the tilt change which leads also to corresponding change in received signal power level. Moreover, the effect of ΔS is seen to be distributed through out the network and has been also exhibited in neighbor areas where those might be served by another antenna. This observed instationarity of shadowing map would unpredictably alter the nature of interference distribution and might introduce inaccuracies while analyzing system performance.

Based on the above observation, investigation has been carried out on the shadowing level change statistics over 63 sectors in order to evaluate how wide through the network and in what range of values does the difference occurs. Statistical results have demonstrated that on average 60% of the pixels reported a shadowing level change in the range of $\pm$1dB when tilt is changed from 2° to 10°. The tendency in the shadow level change have been observed with other tilt setting combinations while small tilt difference yielding less impact. This result is illustrated in Figure 6 where the percentage of pixels experiencing ΔS between $\pm$3dB are presented. Accordingly, it is shown that on average 15% of the pixels have ΔS values out of the $\pm$3dB bound. This percentage is of a significant figure as the statistics is taken from the complete serving network area. Moreover, those pixels which reside in the target sector experience substantial impact from tilting and reflect considerable shadow level change. Figure 5 depicts ΔS in those critical areas of a sector where beam tilt adjustment is required to have predictable impact either in the received signal level or to meet required coverage demand.

VI. Conclusion

In this paper, the impact of antenna tilting on propagation shadowing is thoroughly investigated for urban scenario. Results have demonstrated that changing antenna tilt has a significant impact on the shadowing map. Unlike to the 3GPP assumption, the extracted shadowing map shows existence of its dependency with antenna tilt setting. Furthermore, it has been observed that shadowing maps of different sector antennas on a same sites are far less correlated than the 100% correlation assumption in the current well-established 3GPP models. Therefore, the tilt dependency of shadowing might require a rethinking of currently available propagation models and assumptions.

References

[1] G. Stuber, *Principles of Mobile Communication,3rd Edition*. Springer, 2011.
[2] 3GPP, "Evolved universal terrestrial radio access (E-UTRA); Further advancements for (E-UTRA) physical layer aspects," TR 36.814, Tech. Rep., 2006.
[3] 3GPP, "Evolved universal terrestrial radio access (E-UTRA); Further advancements for (E-UTRA) radio frequency system scenarios," TR 36.942, Tech. Rep., 2009.
[4] E.Huemer and K. Lensing, "Practical antenna guide," KATHREIN MOBILCOM BRASIL Ltda, Tech. Rep., 2000.
[5] L. Thiele, T. Wirth, J. Rumold, and S. Fritze, "Modeling of 3D field patterns of downtilted antennas and their impact on cellular systems," in *International ITG Workshop on Smart Antennas WSA 2009*, Berlin,Germany, February 2009.
[6] W. Lopes, G. Glionna, and M. de Alencar, "Generation of 3D radiation patterns: a geometrical approach," in *IEEE Vehicular Technology Conference*, vol. 2, 2002, pp. 741–744.
[7] F. Giland, A. Claro, J. Ferreira, C. Pardelinha, and L. Correia, "A 3D interpolation method for base-station-antenna radiation patterns," in *IEEE Antennas and Propagation Magazine*, vol. 43, no. 2, April 2001, pp. 132–137.
[8] T. Vasiliadis, A. Dimitriou, and G. Sergiadis, "A novel technique for the approximation of 3-d antenna radiation patterns," in *IEEE Antennas and Propagation Transaction*, vol. 53, no. 7, April 2005, p. 22122219.
[9] 3GPP, "universal terrestrial radio access (UTRA); uplink transmit diversity for high speed packet access," TR 36.814, Tech. Rep., 2010.
[10] G. Wlfle, R.Wahl, P.Wildbolz, and P. Wertz, "Dominant path prediction model for indoor and urban scenarios," AWE Communications, Tech. Rep.
[11] S. Burger, "Accuracy of winprop 3D intelligent ray tracing," AWE Communications, Tech. Rep., 2003.
[12] M. Hata, "Empirical formula for propagation loss in land mobile radio services," in *IEEE Transactions on Vehicular Technology*, vol. 29, no. 3, August 1980, pp. 317–325.
[13] M. Zonoozi and P. Dassanayake, "Shadow fading in mobile radio channel, shadow fading in mobile radio channel," in *Personal, Indoor and Mobile Radio Communications*, vol. 2, August 1996.
[14] Rautiainen, T. Kalliola, and K.Juntunen, "Wideband radio propagation characteristics at 5.3ghz in suburban environments," in *Personal, Indoor and Mobile Radio Communications*, vol. 2, 2005.